AGU ADVANCING EARTH AND SPACE SCIENCE

Geophysical Research Letters

RESEARCH LETTER
10.1029/2022GL101054

A 1000-Year Record of Temperature From Isotopic Analysis of the Deep Critical Zone in Central China

Hongxiu Wang[1,2], Han Li[3], Wei Xiang[4], Yanwei Lu[5], Huanhuan Wang[6], Wei Hu[7], Bingcheng Si[8], Scott Jasechko[9], and Jeffrey J. McDonnell[1,10,11]

[1]School of Environment and Sustainability, Global Institute for Water Security, University of Saskatchewan, Saskatoon, SK, Canada, [2]Key Laboratory of Agricultural Soil and Water Engineering in Arid and Semiarid Areas, Ministry of Education, Northwest A&F University, Yangling, Shaanxi Province, China, [3]Key Research Institute of Yellow River Civilization and Sustainable Development & Collaborative Innovation Center on Yellow River Civilization Jointly Built by Henan Province and Ministry of Education, Henan University, Kaifeng, China, [4]College of Urban and Environmental Sciences, Northwest University, Xi'an, China, [5]Key Laboratory of Subsurface Hydrology and Ecological Effect in Arid Region of Ministry of Education, School of Water and Environment, Chang'an University, Xi'an, China, [6]Shenzhen Water Planning & Design Institute Co., Ltd, Shenzhen, China, [7]The New Zealand Institute for Plant & Food Research Ltd, Christchurch, New Zealand, [8]Department of Soil Science, University of Saskatchewan, Saskatoon, SK, Canada, [9]Bren School of Environmental Science and Management, University of California, Santa Barbara, CA, USA, [10]School of Geography, Earth & Environmental Sciences, University of Birmingham, Birmingham, UK, [11]School of Resources and Environmental Engineering, Ludong University, Yantai, China

Key Points:

- A 98 m "soil core" from the Loess Plateau of China recorded clear paleoclimate information
- δ^2H and $\delta^{18}O$ values of extracted soil water between 14 and 50 m were anomalously low relative to the rest of the core
- The 14–50 m soil pore water bracketed the Little Ice Age period from the years 1420 to 1870

Supporting Information:

Supporting Information may be found in the online version of this article.

Correspondence to:

J. J. McDonnell,
jeffrey.mcdonnell@usask.ca

Citation:

Wang, H., Li, H., Xiang, W., Lu, Y., Wang, H., Hu, W., et al. (2023). A 1000-year record of temperature from isotopic analysis of the deep critical zone in central China. *Geophysical Research Letters*, *50*, e2022GL101054. https://doi.org/10.1029/2022GL101054

Received 29 AUG 2022
Accepted 25 FEB 2023

Abstract Temperature proxies for paleoclimate reconstruction have been made typically via ice cores, tree rings, stalagmites, and lake sediments. While extremely useful, these proxies can be limited spatially. Here we sampled a 98 m "soil core" from Loess Plateau of China and examined the relationship between pore water isotopic values and hydroclimate history. We extracted soil pore water for $\delta^{18}O$, δ^2H, and ^3H and measured chloride concentration. The ^3H-peak at 6 m and chloride mass balance were used to turn depth into calendar year. A 1000 year span was revealed. $\delta^{18}O$ and δ^2H values between 14–50 m were anomalously low—bracketing well the Little Ice Age period from 1420 to 1870. The identification was consistent with other standard proxies in the region and showed the same temporal dynamics of temperature anomalies. Our study shows the potential of stable isotopes of soil water for paleoclimate reconstruction in deep soils.

Plain Language Summary While paleoclimate reconstructions have been made with ice cores, tree rings, lake sediments and other proxies, few if any studies have explored the potential use of soil cores from the unsaturated zone to tease out paleoclimate information. Here, we report the soil water stable isotope data for an unusually deep, unsaturated zone soil core from the Loess Plateau of China. We found that waters extracted from the soil have relatively low δ^2H and $\delta^{18}O$ values in between the depths of 14–50 m. Waters at these depths likely derive from precipitation from the Little Ice Age period that occurred in that region of China from 1420 to 1870. Beyond simple time period identification, our isotope signal also captured the temperature dynamics during the Little Ice Age. We determined this by analyzing pore waters at 20 cm intervals. Tritium (^3H, a radioactive tracer) and a salt mass balance method enabled us to covert core depth increments into calendar year. Our study shows the potential of soil water extractions from the deep critical zone for meaningful interpretation of paleoclimate conditions.

1. Introduction

Paleoclimate reconstructions are critical for understanding the past and for testing models of future climate change. Reconstructions have been done with ice cores (Thompson et al., 2000; Yao & Thompson, 1992), tree rings (Cook et al., 2004; Sheppard et al., 2004), lakebed and ocean floor sediments (Eichler et al., 2011; Mayer & Schwark, 1999; Moberg et al., 2005), and stalagmites (Yang et al., 2002; P. Zhang et al., 2008). However, these proxies can be spatially restricted. One somewhat neglected approach for paleoclimate reconstruction is the geochemical analyses of soil pore waters. There have been some analyses of chloride and tritium for palaeohydrological reconstructions (Edmunds & Tyler, 2002; Stone & Edmunds, 2016). By comparing soil water chloride concentration with deposition amount with wet and dry deposition, the paleo moisture time scales can be determined. Similarly, the depth of the tritium peak in the unsaturated zone relative to the timing of the bomb-peak in 1963 has been used to generate infiltration rates, dates, and flow mechanism (Scanlon et al., 2002; Si and de

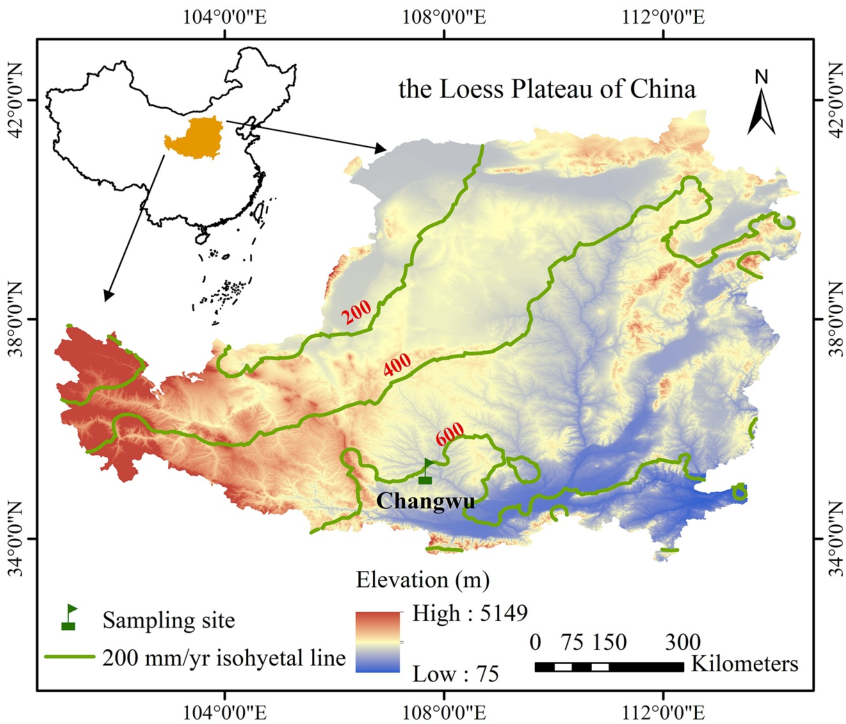

Figure 1. The study area and sampling site. The insert map shows the location of the Loess Plateau in China; the color bar indicates the elevation (m); the green lines are 200 mm/yr isohyetal lines; the green flag indicates our sampling site on the Loess Plateau of China.

Jong, 2007). But to date, δ^2H and $\delta^{18}O$ of soil water have been used primarily as a supplementary tool for paleoclimate work, mostly to reveal discrete cold recharge histories and the extent of evapotranspiration (Hartshough et al., 2001; Tyler et al., 1996). We are not aware of any continuous-with-depth paleoclimate records that have been established via δ^2H and $\delta^{18}O$ of soil water.

Here we sampled the unsaturated zone on the Loess Plateau of China, an exceptionally deep (Li et al., 2020) and potentially rich repository of pore water paleoclimate information. Certainly there has been much work done dating the actual deposits that make up this deep soil (H. Lu et al., 1999; Stevens et al., 2013) and reconstructing paleoclimate using lake sediments, loess, and chloride of the soil pore water (Guo et al., 2022; Huang et al., 2013; Y. Lu et al., 2020; Maher, 2016). Nonetheless, the δ^2H and $\delta^{18}O$ of vadose zone water within these soil deposits—as far as we know—has not been examined for paleoclimate signals.

We focused on an unusually deep (98 m) soil core from the Loess Plateau that includes measurements of $\delta^{18}O$, δ^2H, ^3H, and chloride. We used cryogenic vacuum distillation (Orlowski et al., 2016; Sprenger et al., 2015) to extract the soil water. The main research question driving our study were linked to what paleoclimate period(s) and paleoclimate dates within these period(s) are recorded in the stable isotopic signal of soil water? More specifically, we asked the following questions (a) Can we use tritium to quantify the vertical water migration rate through the deep vadose zone? (b) Can we then convert depth to time to explore how changes in $\delta^{18}O$ and δ^2H of extracted waters correspond to climate events for our measured period? and, (c) Can δ^2H and $\delta^{18}O$ values of soil water capture paleoclimate events bracketed within the time interval of our record?

2. Materials and Methods

2.1. Study Area

The study was conducted in the "Changwu Tableland" located in the southern part of the Loess Plateau of China (Figure 1). The loess deposits of the southern Loess Plateau of China have names associated with their emplacement and have an average thickness of ~100 m (Zhu et al., 2018). The "Wucheng loess" accumulated about 2.5 million years ago, and the "Lishi loess" began to accumulate at about 1.3 million years ago, followed

10.1029/2022GL101054

by the "Malan loess" at 71 thousand years ago (H. Lu et al., 1999). Before and during the Holocene periods, the Loess Plateau of China was dominated by grassland and forest steppe (Shang & Li, 2010). During the last 2000 years, intensive farming accelerated the loss of grassland and natural forest (L. Wang et al., 2006). Since 1990, farmlands were gradually transformed into forest and grassland to combat ecosystem degradation (Su & Fu, 2013). The study area is in a current warm temperate sub-humid zone with an aridity index (precipitation amount/potential evapotranspiration amount) of ∼0.65. The area has a continental monsoon climate with the long term (measured 1957–2020) mean annual temperature, precipitation, and potential evapotranspiration of 9.4 °C, 585 mm, and 897 mm, respectively (Data source: http://cwa.cern.ac.cn/meta/metaData). About 53% of the annual precipitation takes place between July and September. The Changwu Tableland is relatively flat and local agriculture is rain-fed without irrigation.

2.2. Methods

A long-term natural grassland, which was transformed into a non-irrigated wheat field in 2013, was selected as the drilling site for the 98 m soil core. Drilling was completed in 2015. The core was drilled a further 3 m into the saturated zone from 95–98 m using a high-power auger (DPP 100, BJTK Company, CHN). On a nearby wheat/maize rotational farmland site, we drilled an additional 20 m soil core using a hollow-stem hand auger. Considering the potential high isotopic variation and heavy isotope enrichment in the shallow soil, two additional cores (8 and 20 m) were also drilled in 2017 using a hollow-stem hand auger re-sampled next to the original 98 and 20 m soil core sites.

Each of the sampled soil cores were divided into 20 cm length sections. Using the obtained soil samples, soil bulk density, gravimetric water content, soil particle density, and chloride concentration were measured for each of these sections. Soil water was extracted via a cryogenic vacuum distillation system (Li-2000; LICA United Technology Limited, Beijing, China). The extracted soil water was analyzed by isotopic ratio infrared spectroscopy (model IWA-45EP; Los Gatos Research, Inc., San Jose, CA, USA) and a low background liquid scintillation counter (Quantulus 1220, PerkinElmer, Singapore) to obtain stable isotope compositions (δ^2H and δ^{18}O values) and tritium concentrations, respectively. The details of these analytical processes are given in Supporting Information S1 (Text S1).

The ^{3}H-peak and chloride mass balance methods were used to estimate the age of soil water. For the ^{3}H-peak method, we fitted a Gaussian distribution to the ^{3}H-versus-depth profile; the peak of the Gaussian distribution was used to estimate the depth of the ^{3}H peak. Since we know that the ^{3}H input peak—globally and in China—is 1963 (Si and de Jong, 2007), the calendar date of soil water deeper than ^{3}H peak was calculated based on the active root zone method (Equations 1–4; Scanlon et al., 2002):

$$q = \frac{z_p - z_r}{Y_s - 1963}\overline{\theta} \tag{1}$$

where q is the water flux (m year^{-1}), Y_s is sampling year, that is, 2015, $\overline{\theta}$ is the average soil volumetric water content below the active root zone and above the ^{3}H peak (cm^3 cm^{-3}), Z is the soil depth below the surface (m), and the subscript p and r is the ^{3}H peak and active root zone, respectively. Based on water flux and soil volumetric water content, soil pore water velocity (V, m year^{-1}) beneath the tritium peak was obtained.

$$V = \frac{q}{\theta} = \frac{z_p - z_r}{Y_s - 1963}\frac{\overline{\theta}}{\theta} \tag{2}$$

where θ represents soil volumetric water content (cm^3 cm^{-3}). The time (T, year) for displacing the soil water storage to a certain depth was calculated as:

$$T = \frac{\Delta W}{V} = \frac{\int_{Z_p}^{Z} \theta dZ}{(Z_p - Z_r)\overline{\theta}}(Y_s - 1963) \tag{3}$$

where ΔW represents the soil water storage to the certain depth (m). Lastly, the calendar year (Y_Z) for the water at a certain depth was obtained:

$$Y_Z(^3H) = 1963 - \frac{\int_{Z_p}^{Z} \theta dz}{(Z_p - Z_r)\bar{\theta}}(Y_s - 1963) \tag{4}$$

In our study, the active root zone depth was set to 2 m (Y. Lu et al., 2020; Z. Wang et al., 2009; Y. Wang et al., 2015; Xiang et al., 2021), and 1 year residence time for water in the root zone was assumed.

Soil water age, based on chloride mass balance method (Stone & Edmunds, 2016; Tyler et al., 1996), was derived:

$$Y_z(\mathrm{Cl}) = Y_s - \frac{\int_0^z \theta C_s dz}{D} \tag{5}$$

where C_s is the concentration of chloride in soil pore water (mg L^{-1}), D is chloride input flux and was assumed to be 444.9 mg m^{-2} yr^{-1} in our study (Y. Lu et al., 2020). Subsequently, the soil water age was calculated as the average value of ^{3}H-peak and chloride mass balance methods derived ages.

Below the active root zone, we assumed that water moved downward by vertical piston flow and eventually reached the groundwater. The groundwater table at our sampling site was 95 m (Figure 2). Considering 1 m seasonal groundwater fluctuations (R. Wang et al., 2010) and maximum 4 m capillary rise from the water table based on measured grain size (Liu et al., 2014), we focused our analysis on the upper 90 m of soil water to detect any paleoclimate signal. The groundwater δ^2H, δ^{18}O, and ^{3}H data reported here derive from Xiang et al. (2019).

3. Results and Discussion

3.1. Tritium and Chloride Records and the Vertical Water Migration Through the Deep Vadose Zone

Figure 2 shows the extracted soil water ^{3}H profile. It followed a Gaussian distribution with the 1963 bomb peak located at 6.0 ± 0.22 m and the peak ^{3}H concentration of 49 TU. Using the ^{3}H-peak method (Equation 4), the depth from 8–90 m within the soil profile corresponded to a time scale in calendar years, from 764 to 1934 (Figure S1 in Supporting Information S1). We then tested this time estimate using the soil water chloride signal using the chloride mass balance method (Equation 5). The chloride value-to-calendar-year conversion corresponded well to the tritium-based method but shifted the dates slightly to the years 1108–1955 (Figure S2 in Supporting Information S1). We then averaged the soil water age derived from the ^{3}H and chloride methods to obtain the calendar dates of the core from 936 to 1944, for the core length segment from 8 to 90 m (Figure 3).

The basic soil water infiltration perceptual model underpinning the ^{3}H-peak and chloride mass balance method is one-dimensional vertical downward flow. Our data suggest that this perceptual model may be a suitable approximation based on two lines of evidence: (a) the groundwater stable isotope value was very close to the mean 8–90 m soil water stable isotope value, and (b) the tritium concentration of groundwater was very low (Figure 2) indicating that no recent precipitation water moves downward via preferential flow. Therefore, piston downward flow appears to be the primary water movement process. Further, our perception of downward displacement is consistent with other research on the Loess Plateau of China (Huang et al., 2017; Xiang et al., 2019).

3.2. How Changes in δ^{18}O and δ^2H of Extracted Waters Correspond to Notable Climate Events?

The extracted soil water δ^2H and δ^{18}O showed similar vertical profiles, with higher values at depths shallower than 2 m and variable values between 8 and 90 m depth (Figure 2). The isotopic composition of shallow soil water in the depth range of 0–8 m exhibited large variations and the variation decreased with increasing soil depth. To avoid the uncertainty caused by these large isotopic variations at depths shallower than 8 m, we focused our paleoclimate analyses exclusively on soil waters from 8 to 90 m. We compared δ^2H and δ^{18}O of soil water with the 8–90 m mean isotopic value (−9.7‰ for δ^{18}O, and −72.5‰ for δ^2H). We used two sigma (2‰ for δ^2H and 0.4‰ for δ^{18}O) analysis precision to quantify the isotopic difference through the core. Any soil water δ^{18}O or δ^2H values that differed from the mean value by less than the two sigma analytical precision was defined as "minimal difference." Groundwater with −72.7‰ and −10.1‰ for δ^2H and δ^{18}O were similar to the 8–90 m mean isotopic value. But notably, a zone from 14 to 50 m was detected as a heavy isotope depletion anomaly, which plotted below the 8–90 m mean line (Figure 3).

The sustained below-average isotope values between 14 and 50 m mapped to the time period of 1420–1870 (Figure 3) and is evidence of the Little Ice Age preserved in our core. Therefore, our overall core can be divided

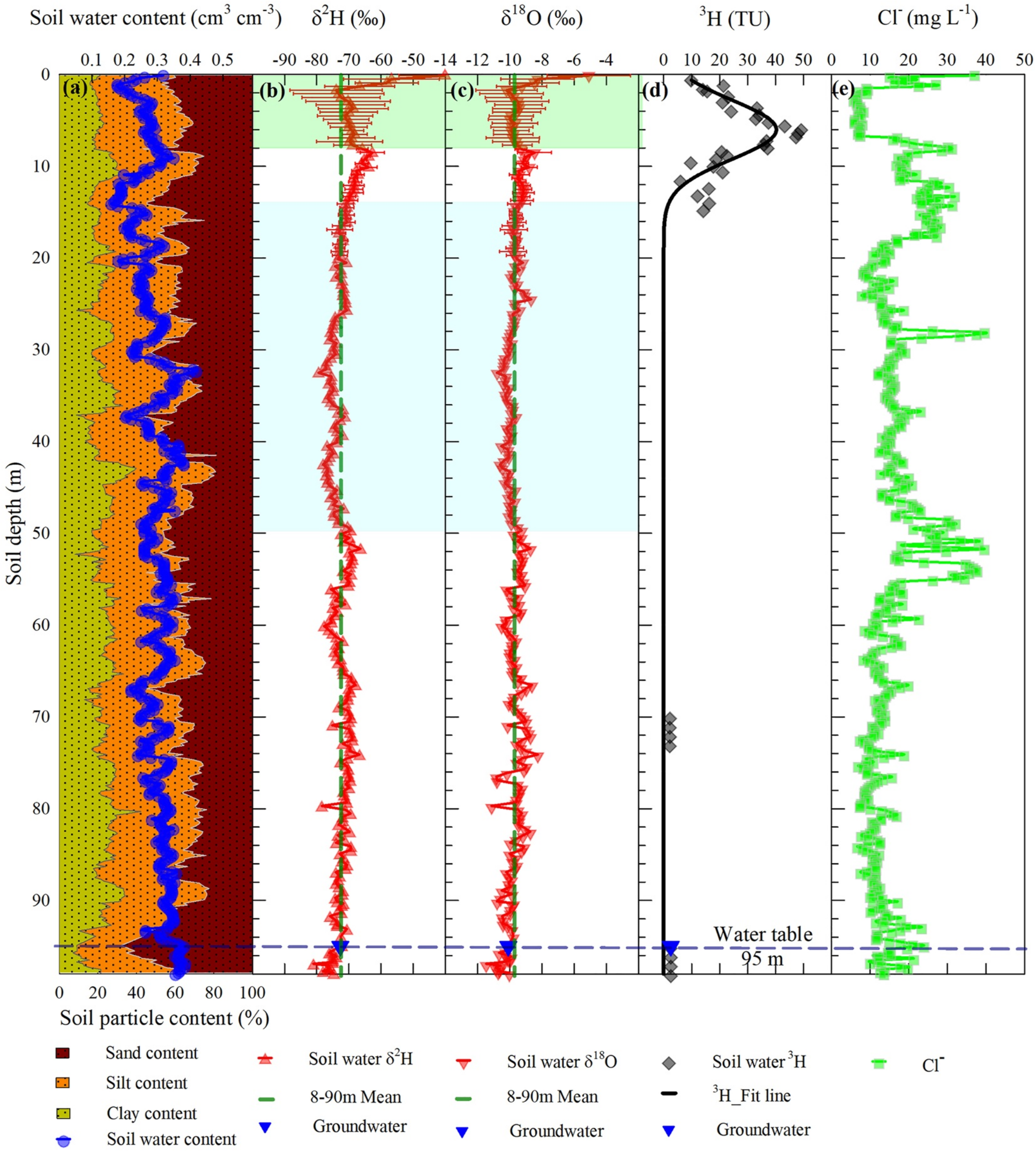

Figure 2. The vertical distribution of soil particle content, water content (a), and soil water and groundwater δ^2H (b), $\delta^{18}O$ (c), ^3H (d), and Cl^- (e). Green, orange, and red shaded areas represent clay, silt, and sand content, respectively. The blue circles, red upward-triangles, red downward-triangles, gray diamonds, green squares, and blue downward-triangles show soil volumetric water content, δ^2H, $\delta^{18}O$, ^3H, Cl^-, and isotopic composition of groundwater respectively. The vertical green dashed lines are the 8–90 m mean δ^2H and $\delta^{18}O$ values. The black line shows the Gaussian distribution fitted to the ^3H vertical profile. The blue dashed line indicates the groundwater table. The ^3H-peak is located at 6.0 ± 0.22 m with a concentration of 49 TU. δ^2H and $\delta^{18}O$ show large variations for the upper 8 m and oscillate around the mean value of the 8–90 m (−9.7‰ for $\delta^{18}O$, and −72.5‰ for δ^2H) for the deeper soil.

into three periods: 936–1420 (around average), 1420–1870 (below average), and 1870–1944 (above average with an increasing trend). These periods before and after the bracketed Little Ice Age, we believe, map directly to the Medieval Warm Period (i.e., the period before the Little Ice Age) and the Current Warm Period, the period after ~1870 (Chen et al., 2006).

3.3. Other Evidence to Support That Soil Water Between 14 and 50 m Is Little Ice Age Water

Our estimated Little Ice Age timing could be affected by how we chose the "average line" in Figure 3. To check the reliability of this timing (starting in 1420 and ending in 1870), we extracted independently, the time period

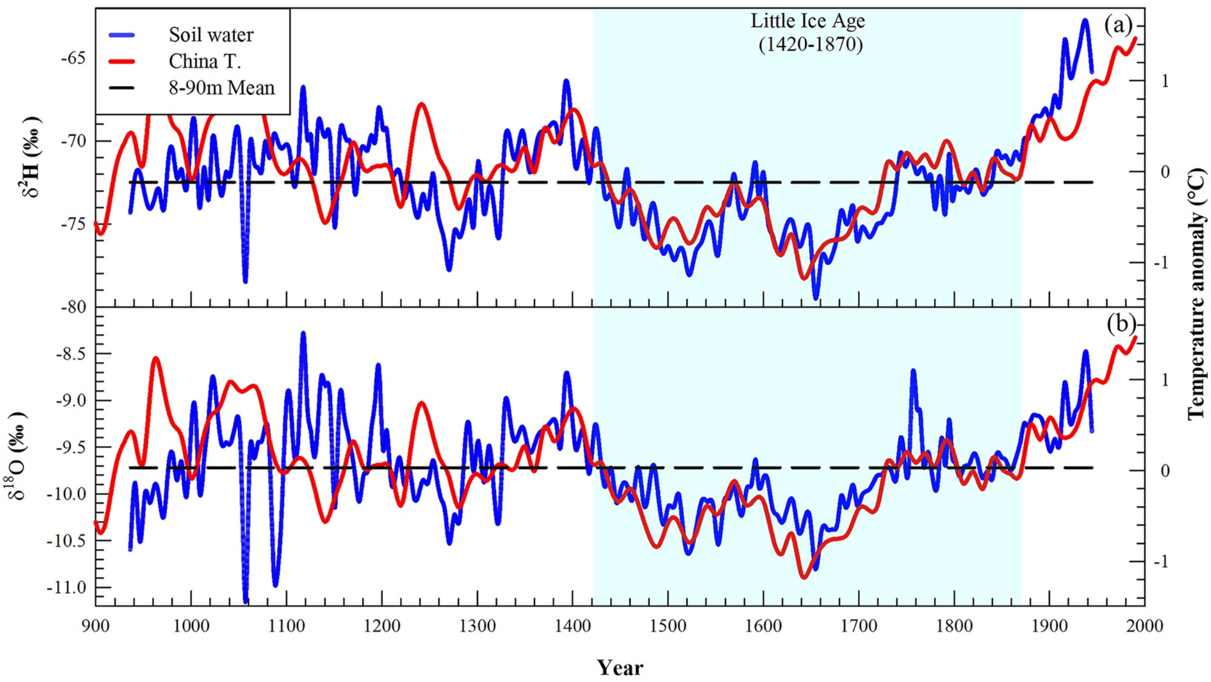

Figure 3. Temporal variation in soil water δ^2H (a) and δ^{18}O (b). The blue lines represent the measured soil water data dated by the ^{3}H-peak and chloride mass balance methods; the temperature anomaly in China is shown in the red lines based on Yang et al. (2002). The black dashed lines represent the 8–90 m mean isotopic values. The soil water zone in the range 8–90 m was converted to calendar years 936–1944 using the average date from ^{3}H-peak and chloride mass balance methods. Sustained, below average isotope values in the 14–50 m soil zone brackets the Little Ice Age from 1420 to 1870. During the Little Ice Age, δ^2H and δ^{18}O show very similar temporal dynamics to the temperature anomaly data in China.

from text descriptions in published literature using other proxies near our sampling site. Table 1 shows the strong agreement with these other sources and our bracketed time for the Little Ice Age. Work with the δ^{18}O of the "Dunde ice core," 1,400 km from our site, suggests that the Little Ice Age spanned the years 1360–1840 (Yao & Thompson, 1992). The "Dulan tree ring" index, determined 880 km from our site, suggests that the Little Ice Age took place there from 1450 to 1820 (Q. Zhang et al., 2003). Stalagmite δ^{18}O data reported for the Wanxiang Cave, 325 km from our site (P. Zhang et al., 2008), placed the Little Ice Age dates between 1350 and 1900. Sediment δ^{18}O and δ^{13}C of the "Lake Ebinur," 2,360 km from our site, bracketed the Little Ice Age dates between 1400 and 1750 (Ma et al., 2011). Larger scale analysis placed the Little Ice Age from 1400 to 1920 in China, generally (Yang et al., 2002). Collectively, these data show a starting year that varies from 1350 to 1450 and ending between 1750 and 1920. Our estimated time period, from the start of 1420 to the end of 1870, is within the range of the regional reported times reinforcing the capability of our method for paleoclimatic reconstruction.

During the Little Ice Age, our isotope signal further captured the temperature dynamics within this period. The δ^2H values (which follow similar patterns to δ^{18}O values) and temperatures in China both decreased over time from 1420 to 1520, followed by an increasing trend until 1600, and then a decrease to their lowest values at 1660. This was followed by increases until 1740, followed by a stable period between 1740 and 1870 (Figure 3).

Table 1
The Time Period of Little Ice Age From the Published Literature

Author	Location	Latitude	Longitude	Proxy	Time period
Our study	Changwu (China)	35°14′N	107°41′E	Unsaturated soil zone δ^2H and δ^{18}O	1420–1870
Yao and Thompson (1992)	Dunde (China)	38°06′N	92°24′E	Ice core δ^{18}O	1360–1840
Zhang et al. (2003)	Dulan (China)	36°20′N	98°00′E	Tree ring width	1450–1820
Zhang et al. (2008)	Wanxiang (China)	33°19′N	105°00′E	Stalagmite δ^{18}O	1350–1900
Ma et al. (2011)	Lake Ebinur (China)	45°01′N	82°52′E	Lake sediment δ^{18}O, δ^{13}C	1400–1750
Yang et al. (2002)	China	Ice cores, tree rings, lake sediments, and historical documents			1400–1920

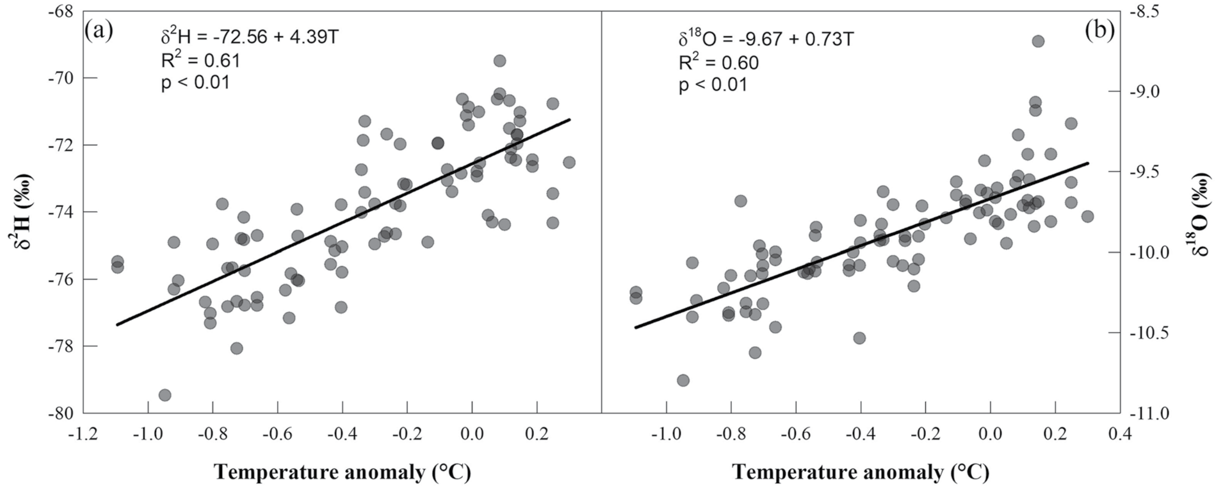

Figure 4. The correlation of soil water δ^2H (a) and δ^{18}O (b) with the temperature anomaly in China (Yang et al., 2002) during the Little Ice Age. The positive correlation is significant ($p < 0.01$).

Furthermore, soil water δ^2H and δ^{18}O showed significant positive correlation with reported temperature anomalies in China ($p < 0.01$; Figure 4). Higher temperatures produced higher δ^2H and δ^{18}O values, and lower temperatures resulted in lower δ^2H and δ^{18}O values in soil water during the Little Ice Age. On balance, our isotope proxy from soil water extractions in the deep critical zone at our site recorded both the sustained cold signal timescale and also the major temperature trends during the Little Ice Age.

The Little Ice Age shows regional coherence but does not occur at the same time globally (Neukom et al., 2019). Our study indicated that the Loess Plateau experienced cold periods between 1420 and 1870 with an average resolution of ∼3 yr/sample. The cold conditions could be related to the decreasing solar activity, the weakening of the East Asian summer monsoon, and/or intensifies of East Asian winter monsoon (Guo et al., 2022; Wanner et al., 2008). Our high-resolution sampling method may contribute to a robust paleoclimate reconstruction compared with other low sampling resolution methods on the Loess Plateau, such as the loess itself, which has a temporal resolution of ∼500 yr/sample (Kang et al., 2018; Maher, 2016).

3.4. Uncertainties and Issues for Using Soil Water δ^2H and δ^{18}O to Reveal Little Ice Age Climate

Our data suggest that soil water δ^2H and δ^{18}O can be used to reveal the Little Ice Age on the Loess Plateau of China. δ^2H and δ^{18}O of soil water are determined by the isotopic values of precipitation, which is driven by moisture provenance, air mass trajectories and mixing, and atmospheric temperatures (Dansgaard, 1964; Kirchenbaum, 1951). The isotopic values are also affected by soil evaporation, which is driven by temperature and relative humidity (Allison, 1982). When temperatures are low, soil evaporation can be suppressed, and isotopic compositions of soil water can capture those of precipitation. Therefore, soil water δ^2H and δ^{18}O values are lower during the Little Ice Age. Precipitation δ^2H and δ^{18}O values can also be lower during large rain events at some tropical and subtropical locations (Jasechko & Taylor, 2015). However, δ^2H and δ^{18}O values of soil water show no relationship with chloride concentration (which has negative correlation with rain amount) during the Little Ice Age (figure not shown) suggesting that the lower δ^2H and δ^{18}O values are not produced by large rain events. Collectively, soil water δ^2H and δ^{18}O can be used as proxies for paleoclimate reconstruction. The positive correlation of δ^2H and δ^{18}O values of soil water with temperature during the Little Ice Age needs to be validated in other areas with deep soil profiles. The length of time captured by unsaturated zone waters is likely to be longer in areas where downward soil water flow rates are slow and where soils are thick (Edmunds & Tyler, 2002; Stone & Edmunds, 2016), suggesting further deep vadose zone water extractions should be done in arid and sub-humid areas with soil thickness exceeding 50 m to capture paleoclimate conditions (e.g., the Pampas in Argentina; see Li et al., 2020; Montoya et al., 2019; Teruggi, 1957; Zárate, 2003).

4. Conclusions

A 98 m soil core that included 95 m of unsaturated zone and 3 m of saturated zone was extracted to obtain soil water δ^2H, δ^{18}O, ^{3}H, and chloride. ^{3}H-peak and chloride mass balance methods were able to be used to convert soil depths to calendar time. By comparing the isotopic composition of soil water at 20 cm intervals through the core with the mean isotopic values between 8 and 90 m, a period of sustained low δ^2H and δ^{18}O values was observed between 14 and 50 m, corresponding to the years 1420–1870. This Little Ice Age period revealed by soil water extractions from our deep core was consistent with other local and more traditional climate proxies. In addition, the isotopic compositions of soil water captured the dynamic of regional reconstructed paleotemperature within Little Ice Age. We offer these findings as encouragement to others to explore for other deep critical zones, the hitherto unexplored signals in extracted soil waters.

Conflict of Interest

The authors declare no conflicts of interest relevant to this study.

Data Availability Statement

The isotopes and chloride concentration data used for converting soil sampling depth to calendar year and revealing the Little Ice Age period are available in the Federated Research Data Repository at H. Wang et al. (2022), https://doi.org/10.20383/103.0628.

Acknowledgments
This research has been supported by the Natural Sciences and Engineering Research Council of Canada (Discovery Grant to JJM), the Major Scientific and Technological Innovation Projects of Shandong Key R & D Plan (Grant 2019JZZY010710), and Shandong Province "International Research Team Building Plan" Program. We thank the 3 reviewers for their very useful suggestions on how to improve the manuscript.

References

Allison, G. B. (1982). The relationship between ^{18}O and deuterium in water in sand columns undergoing evaporation. *Journal of Hydrology*, *55*(1–4), 163–169. https://doi.org/10.1016/0022-1694(82)90127-5

Chen, F., Huang, X., Zhang, J., Holmes, J. A., & Chen, J. (2006). Humid little ice age in arid central Asia documented by Bosten Lake, Xinjiang, China. *Science in China—Series D: Earth Sciences*, *49*(12), 1280–1290. https://doi.org/10.1007/s11430-006-2027-4

Cook, E. R., Esper, J., & D'Arrigo, R. D. (2004). Extra-tropical northern hemisphere land temperature variability over the past 1000 years. *Quaternary Science Reviews*, *23*(20–22), 2063–2074. https://doi.org/10.1016/j.quascirev.2004.08.013

Dansgaard, W. (1964). Stable isotopes in precipitation. *Tellus*, *16*(4), 436–468. https://doi.org/10.1111/j.2153-3490.1964.tb00181.x

Edmunds, W., & Tyler, S. (2002). Unsaturated zones as archives of past climates: Toward a new proxy for continental regions. *Hydrogeology Journal*, *10*(1), 216–228. https://doi.org/10.1007/s10040-001-0180-6

Eichler, A., Tinner, W., Brütsch, S., Olivier, S., Papina, T., & Schwikowski, M. (2011). An ice-core based history of Siberian forest fires since AD 1250. *Quaternary Science Reviews*, *30*(9–10), 1027–1034. https://doi.org/10.1016/j.quascirev.2011.02.007

Guo, C., Ma, Y., & Meng, H. (2022). Late Holocene vegetation, climate, and lake changes in northern China: Varved evidence from western Loess Plateau. *Science of The Total Environment*, *827*, 154282. https://doi.org/10.1016/j.scitotenv.2022.154282

Hartsough, P., Tyler, S. W., Sterling, J., & Walvoord, M. (2001). A 14.6 Kyr record of nitrogen flux from desert soil profiles as inferred from vadose zone pore waters. *Geophysical Research Letters*, *28*(15), 2955–2958. https://doi.org/10.1029/2000gl011823

Huang, T., Pang, Z., & Edmunds, W. M. (2013). Soil profile evolution following land-use change: Implications for groundwater quantity and quality. *Hydrological Processes*, *27*(8), 1238–1252. https://doi.org/10.1002/hyp.9302

Huang, T., Pang, Z., Liu, J., Ma, J., & Gates, J. (2017). Groundwater recharge mechanism in an integrated tableland of the Loess Plateau, northern China: Insights from environmental tracers. *Hydrogeology Journal*, *25*(7), 2049–2065. https://doi.org/10.1007/s10040-017-1599-8

Jasechko, S., & Taylor, R. G. (2015). Intensive rainfall recharges tropical groundwaters. *Environmental Research Letters*, *10*(12), 124015. https://doi.org/10.1088/1748-9326/10/12/124015

Kang, S., Wang, X., Roberts, H. M., Duller, G. A., Cheng, P., Lu, Y., & An, Z. (2018). Late Holocene anti-phase change in the East Asian summer and winter monsoons. *Quaternary Science Reviews*, *188*, 28–36. https://doi.org/10.1016/j.quascirev.2018.03.028

Kirschenbaum, I. (1951). *Physical properties and analysis of heavy water* (Vol. 438). McGraw-Hill. https://doi.org/10.1126/science.115.2990.428

Li, Y., Shi, W., Aydin, A., Beroya-Eitner, M. A., & Gao, G. (2020). Loess genesis and worldwide distribution. *Earth-Science Reviews*, *201*, 102947. https://doi.org/10.1016/j.earscirev.2019.102947

Liu, Q., Yasufuku, N., Miao, J., & Ren, J. (2014). An approach for quick estimation of maximum height of capillary rise. *Soils and Foundations*, *54*(6), 1241–1245. https://doi.org/10.1016/j.sandf.2014.11.017

Lu, H., Liu, X., Zhang, F., An, Z., & Dodson, J. (1999). Astronomical calibration of loess–paleosol deposits at Luochuan, central Chinese Loess Plateau. *Palaeogeography, Palaeoclimatology, Palaeoecology*, *154*(3), 237–246. https://doi.org/10.1016/s0031-0182(99)00113-3

Lu, Y., Li, H., Si, B., & Li, M. (2020). Chloride tracer of the loess unsaturated zone under sub-humid region: A potential proxy recording high-resolution hydroclimate. *Science of The Total Environment*, *700*, 134465. https://doi.org/10.1016/j.scitotenv.2019.134465

Ma, L., Wu, J., Yu, H., Zeng, H., & Jilili, A. (2011). The medieval warm period and the little ice age from a sediment record of Lake Ebinur, northwest China. *Boreas*, *40*(3), 518–524. https://doi.org/10.1111/j.1502-3885.2010.00200.x

Maher, B. A. (2016). Palaeoclimatic records of the loess/palaeosol sequences of the Chinese Loess Plateau. *Quaternary Science Reviews*, *154*, 23–84. https://doi.org/10.1016/j.quascirev.2016.08.004

Mayer, B., & Schwark, L. (1999). A 15,000-year stable isotope record from sediments of Lake Steisslingen, Southwest Germany. *Chemical Geology*, *161*(1–3), 315–337. https://doi.org/10.1016/s0009-2541(99)00093-5

Moberg, A., Sonechkin, D. M., Holmgren, K., Datsenko, N. M., & Karlén, W. (2005). Highly variable Northern Hemisphere temperatures reconstructed from low-and high-resolution proxy data. *Nature*, *433*(7026), 613–617. https://doi.org/10.1038/nature03265

Montoya, J. C., Porfiri, C., Roberto, Z. E., & Viglizzo, E. F. (2019). Assessing the vulnerability of groundwater resources in semiarid lands of central Argentina. *Sustainable Water Resources Management*, *5*(4), 1419–1434. https://doi.org/10.1007/s40899-018-0246-4

Neukom, R., Steiger, N., Gómez-Navarro, J. J., Wang, J., & Werner, J. P. (2019). No evidence for globally coherent warm and cold periods over the preindustrial common era. *Nature*, *571*(7766), 550–554. https://doi.org/10.1038/s41586-019-1401-2

Orlowski, N., Pratt, D. L., & McDonnell, J. J. (2016). Intercomparison of soil pore water extraction methods for stable isotope analysis. *Hydrological Processes*, *30*(19), 3434–3449. https://doi.org/10.1002/hyp.10870

Scanlon, B. R., Healy, R. W., & Cook, P. G. (2002). Choosing appropriate techniques for quantifying groundwater recharge. *Hydrogeology Journal*, *10*(1), 18–39. https://doi.org/10.1007/s10040-002-0200-1

Shang, X., & Li, X. (2010). Holocene vegetation characteristics of the southern Loess Plateau in the Weihe River valley in China. *Review of Palaeobotany and Palynology*, *160*(1–2), 46–52. https://doi.org/10.1016/j.revpalbo.2010.01.004

Sheppard, P. R., Tarasov, P. E., Graumlich, L. J., Heussner, K. U., Wagner, M., Österle, H., & Thompson, L. G. (2004). Annual precipitation since 515 BC reconstructed from living and fossil juniper growth of northeastern Qinghai Province, China. *Climate Dynamics*, *23*(7), 869–881. https://doi.org/10.1007/s00382-004-0473-2

Si, B. C., & de Jong, E. (2007). Determining long-term (decadal) deep drainage rate using multiple tracers. *Journal of Environmental Quality*, *36*(6), 1686–1694. https://doi.org/10.2134/jeq2007.0029

Sprenger, M., Herbstritt, B., & Weiler, M. (2015). Established methods and new opportunities for pore water stable isotope analysis. *Hydrological Processes*, *29*(25), 5174–5192. https://doi.org/10.1002/hyp.10643

Stevens, T., Adamiec, G., Bird, A. F., & Lu, H. (2013). An abrupt shift in dust source on the Chinese Loess Plateau revealed through high sampling resolution OSL dating. *Quaternary Science Reviews*, *82*, 121–132. https://doi.org/10.1016/j.quascirev.2013.10.014

Stone, A. E. C., & Edmunds, W. M. (2016). Unsaturated zone hydrostratigraphies: A novel archive of past climates in dryland continental regions. *Earth-Science Reviews*, *157*, 121–144. https://doi.org/10.1016/j.earscirev.2016.03.007

Su, C., & Fu, B. (2013). Evolution of ecosystem services in the Chinese Loess Plateau under climatic and land use changes. *Global and Planetary Change*, *101*, 119–128. https://doi.org/10.1016/j.gloplacha.2012.12.014

Teruggi, M. E. (1957). The nature and origin of Argentine loess. *Journal of Sedimentary Research*, *27*(3), 322–332. https://doi.org/10.1306/74d706dc-2b21-11d7-8648000102c1865d

Thompson, L. G., Yao, T., Mosley-Thompson, E., Davis, M. E., Henderson, K. A., & Lin, P. N. (2000). A high-resolution millennial record of the South Asian monsoon from Himalayan ice cores. *Science*, *289*(5486), 1916–1919. https://doi.org/10.1126/science.289.5486.1916

Tyler, S. W., Chapman, J. B., Conrad, S. H., Hammermeister, D. P., Blout, D. O., Miller, J. J., et al. (1996). Soil-water flux in the southern Great Basin, United States: Temporal and spatial variations over the last 120,000 years. *Water Resources Research*, *32*(6), 1481–1499. https://doi.org/10.1029/96wr00564

Wang, H., Li, H., Xiang, W., Lu, Y., Wang, H., Hu, W., et al. (2022). A 1000-yr record of temperature from isotopic analysis of the deep critical zone in central China. *Federated Research Data Repository*. https://doi.org/10.20383/103.0628

Wang, L., Shao, M. A., Wang, Q., & Gale, W. J. (2006). Historical changes in the environment of the Chinese Loess Plateau. *Environmental Science & Policy*, *9*(7–8), 675–684. https://doi.org/10.1016/j.envsci.2006.08.003

Wang, R., Liu, W. Z., & Zhao, X. P. (2010). Dynamic characteristics of groundwater level on Changwu tableland. *Agricultural Research in the Arid Areas*, *28*, 48–52. https://doi.org/10.1017/S0004972710001772

Wang, Y., Hu, W., Zhu, Y., Shao, M. A., Xiao, S., & Zhang, C. (2015). Vertical distribution and temporal stability of soil water in 21-m profiles under different land uses on the Loess Plateau in China. *Journal of Hydrology*, *527*, 543–554. https://doi.org/10.1016/j.jhydrol.2015.05.010

Wang, Z., Liu, B., & Zhang, Y. (2009). Soil moisture of different vegetation types on the Loess Plateau. *Journal of Geographical Sciences*, *19*(6), 707–718. https://doi.org/10.1007/s11442-009-0707-7

Wanner, H., Beer, J., Bütikofer, J., Crowley, T. J., Cubasch, U., Flückiger, J., et al. (2008). Mid-to late Holocene climate change: An overview. *Quaternary Science Reviews*, *27*(19–20), 1791–1828. https://doi.org/10.1016/j.quascirev.2008.06.013

Xiang, W., Si, B., Li, M., Li, H., Lu, Y., Zhao, M., & Feng, H. (2021). Stable isotopes of deep soil water retain long-term evaporation loss on China's Loess Plateau. *Science of The Total Environment*, *784*, 147153. https://doi.org/10.1016/j.scitotenv.2021.147153

Xiang, W., Si, B. C., Biswas, A., & Li, Z. (2019). Quantifying dual recharge mechanisms in deep unsaturated zone of Chinese Loess Plateau using stable isotopes. *Geoderma*, *337*, 773–781. https://doi.org/10.1016/j.geoderma.2018.10.006

Yang, B., Braeuning, A., Johnson, K. R., & Yafeng, S. (2002). General characteristics of temperature variation in China during the last two millennia. *Geophysical Research Letters*, *29*(9), 38–1. https://doi.org/10.1029/2001gl014485

Yao, T., & Thompson, L. G. (1992). Trends and features of climatic changes in the past 5000 years recorded by the Dunde ice core. *Annals of Glaciology*, *16*, 21–24. https://doi.org/10.1017/s0260305500004766

Zárate, M. A. (2003). Loess of southern south America. *Quaternary Science Reviews*, *22*(18–19), 1987–2006. https://doi.org/10.1016/s0277-3791(03)00165-3

Zhang, P., Cheng, H., Edwards, R. L., Chen, F., Wang, Y., Yang, X., et al. (2008). A test of climate, sun, and culture relationships from an 1810-year Chinese cave record. *Science*, *322*(5903), 940–942. https://doi.org/10.1126/science.1163965

Zhang, Q. B., Cheng, G., Yao, T., Kang, X., & Huang, J. (2003). A 2,326-year tree-ring record of climate variability on the northeastern Qinghai-Tibetan Plateau. *Geophysical Research Letters*, *30*(14), 1739. https://doi.org/10.1029/2003gl017425

Zhu, Y., Jia, X., & Shao, M. (2018). Loess thickness variations across the Loess Plateau of China. *Surveys in Geophysics*, *39*(4), 715–727. https://doi.org/10.1007/s10712-018-9462-6

References From the Supporting Information

Gaj, M., Kaufhold, S., & McDonnell, J. J. (2017). Potential limitation of cryogenic vacuum extractions and spiked experiments. *Rapid Communications in Mass Spectrometry*, *31*(9), 821–823. https://doi.org/10.1002/rcm.7850

Lu, Y., Si, B., Li, H., & Biswas, A. (2019). Elucidating controls of the variability of deep soil bulk density. *Geoderma*, *348*, 146–157. https://doi.org/10.1016/j.geoderma.2019.04.033

Wang, H., Si, B., & Li, M. (2018). Distribution of hydrogen and oxygen isotopes along deep soil profiles in a loess tableland. *Journal of Irrigation and Drainage*, *37*(12), 53–59. https://doi.org/10.13522/j.cnki.ggps.20180195

Wen, M., Lu, Y., Li, M., He, D., Xiang, W., Zhao, Y., et al. (2021). Correction of cryogenic vacuum extraction biases and potential effects on soil water isotopes application. *Journal of Hydrology*, *603*, 127011. https://doi.org/10.1016/j.jhydrol.2021.127011